

Local statistics of immiscible and incompressible two-phase flow in porous media

Hursanay Fyhn,^{1,*} Santanu Sinha,^{2,†} and Alex Hansen^{1,‡}

¹*PoreLab, Department of Physics, Norwegian University of Science and Technology, NTNU, N-7491 Trondheim, Norway*

²*PoreLab, Department of Physics, University of Oslo, N-0316 Oslo, Norway*

(Dated: March 2, 2023)

We consider immiscible and incompressible two-phase flow in porous media under steady-state conditions using a dynamic pore network model. We focus on the fluctuations in a Representative Elementary Area (REA), with the aim to demonstrate that the statistical distributions of the volumetric flow rate and the saturation within the REA become independent of the size of the entire model when the model is large enough. This independence is a necessary condition for developing a local statistical theory for the flow, which in turn opens for the possibility to formulate a description at scales large enough for the typical pore size to be negligible using differential equations.

PACS numbers:

I. INTRODUCTION

When two or more immiscible fluids compete for space while flowing in a porous medium, we are dealing with multiphase flow [1–4]. Finding a proper description of multiphase flow at the Darcy scale, which may be orders of magnitude larger than the pore scale, is a central problem in porous media research. On the Darcy scale, the only practical approach to the multiphase flow problem is to replace the original porous medium with a continuous medium and then describe the flow through a set of differential equations relating the fluid velocities to the driving forces, e.g. pressure gradients, saturation gradients and gravity. The approach dominating any practical applications of immiscible two-phase flow that today requires calculations is based on relative permeability theory [5]. This is a purely phenomenological theory essentially stating that the two immiscible fluids get into each other way and therefore reduce the effective permeability each fluid experiences. Add a capillary pressure function to take into account the capillary forces between the two fluids, and the theory is complete [6]. This phenomenological approach has the flaw that it provides no path to implement into it our increasing understanding of the interactions and flow of the fluids at both the pore scale and the molecular scale.

Solving the *scale-up problem* in immiscible two-phase flow in porous media consists of expressing the flow at the pore scale in terms of the flow at the molecular scale and then expressing the flow at the Darcy scale in terms of the flow at the pore scale. The favored approach to the scale-up problem is that of homogenization. That is, start with a description of the problem on small scale using variables appropriate for that scale. Then average these variables over the large scale, followed by closure assumptions.

One example of the homogenization approach of scaling up immiscible two-phase flow in porous media starts from mechanical principles such as momentum conservation to arrive at an effective description of the flow through homogenization [7–12]. Thermodynamically Constrained Averaging Theory (TCAT) [13–18] is a very different approach to the scale-up problem. It is based on volume averages of thermodynamic quantities defined at the sub-pore and pore scale, together with closure relations at the homogeneous scale as formulated by Whitaker [7]. Another homogenization approach is that of Kjelstrup et al. [19–21], who use Euler scaling to work out the averages of intensive variables such as pressure. This approach manages to keep the number of variables down in contrast to other approaches. We also point to the homogenization approach based on expressing the central thermodynamic potentials in terms of geometric variables that characterize the porous medium, the fluid interfaces and the contact lines and the Minkowski functionals combined with powerful theorems from differential geometry [22–25].

These homogenization approaches succeed in taking the description of the flow from the sub-pore scale to scales just above the pore scale. They do not, however, take into account the fluid structures that appear at even larger scales. These structures result from the way the fluids arrange themselves within the porous medium, i.e., their cluster structure. They profoundly affect the flow on the intermediate scales below the Darcy scale — and this must be reflected in the flow at the Darcy scale. Energetically, these structures are not dominating, and therefore easy to discard in the different homogenization approaches. However, any scale-up attempt taking the problem from the pore scale to the Darcy scale needs to take these structures into account. As the structures appear over many length scales, a different approach from those based on homogenization techniques is needed.

Looking back in history, there is an upscaling technique that is capable of dealing with structures and correlations that stretch across scales: statistical mechanics [26]. The early developers of thermodynamics constructed their approach in order to understand heat and its relation to

*Electronic address: hursanay.fyhn@ntnu.no

†Electronic address: santanu.sinha@ntnu.no

‡Electronic address: alex.hansen@ntnu.no

work in parallel to the development of the steam engine. It is based on conservation laws and symmetries, especially dilation symmetry. It treats the medium as a continuum and provides the necessary differential equations. Statistical mechanics was developed to understand how the motion of atoms and molecules leads to the thermodynamic relations, i.e., it provides the scaling up from the molecular scale to the continuum scale, thus circumventing the necessity to solve the equations of motion for every molecule.

One may therefore get the impression that thermodynamics and statistical mechanics are inextricably linked to atomic and molecular systems. This is, however, not correct. Jaynes [27] developed a generalized statistical mechanics in the fifties based on the statistical approach to information developed by Shannon a few years earlier [28]. This approach, in turn, originates in the *principle of sufficient reason* formulated by Laplace [29]: If we know nothing about a process with two outcomes, the optimal choice of probabilities for the two outcomes is 50 % for each. Shannon constructed a *function of ignorance* measuring quantitatively what we do *not* know about a given process having a number of different outcomes. One of his criteria for this function, called the Shannon entropy, was that it would have its maximum value when the probabilities for all outcomes would be equal, which is a generalization of the Laplace principle of sufficient reason. Jaynes took this approach further by adding the criterion that the Shannon entropy is maximum given what is known about the process. This leads to a set of equations that determine the probabilities for the different outcomes. This is Jaynes’ generalization of statistical mechanics.

An important caveat in applying the Jaynes maximum entropy approach is that it does not work for driven systems [30]. Immiscible two-phase flow in porous media does represent a driven system where there is production of entropy due to viscous dissipation and irreversible motion of fluid interfaces and contact lines. Nevertheless, in a recent paper, Hansen et al. [31] developed a statistical mechanics for immiscible and incompressible two-phase flow in porous media based on the Jaynes principle of maximum entropy, leading to a formalism resembling thermodynamics that describes the flow at the continuum level. The trick to make it work was not to consider the molecular entropy which is being produced when the fluids move, but rather the entropy associated with the flow patterns of the fluids. This entropy is *not* being produced under steady-state flow conditions. Furthermore, it is this entropy that properly describes the fluid structures on scales above the pore scale, whereas the molecular entropy associated with dissipation dominates at scales up to the pore scale.

The Jaynes approach solves the scale-up problem in the same way as it was solved through ordinary statistical mechanics for atomistic systems. It is the aim of the present paper to investigate numerically a necessary criterion which was only assumed to be true in [31] for

the Jaynes approach to be applicable to immiscible two-phase flow in porous media: can we partition the porous medium into a “system” in contact with a “reservoir” as in ordinary thermodynamics? The term “reservoir” has very different meanings in thermodynamics and in porous media research. In this work, the term is used in a thermodynamical sense, which is that a reservoir is a system large enough so that the variables describing it do not change when brought into contact with a system small enough for its variables to be affected. The way we answer the question just posed is this: Based on a numerical model, we record the statistics of key parameters in the system for different sizes of the reservoir, finding that the statistics is independent of the reservoir size when it is large enough.

We note that there have been earlier attempts at capturing the evolution of retention in unsaturated porous media subject to quasi-static changes in imposed pressure. Xu and Louge [32] formulate drainage or imbibition through porous media using an Ising model that predicts the retention curve of saturation vs capillary pressure. This is a very different approach with different aims from that of Hansen et al. [31] who focus on steady-state flow.

We will in the following relate the concept of a “system” to that of a *Representative Elementary Area* (REA) [33]. At each point in the pore space of the porous medium, we may place an area that is orthogonal to the streamline passing through it. The area qualifies as an REA if it is large enough for the variables describing the properties of the medium itself and the fluids passing through it to have well-defined averages. To obtain meaningful averages, the length scale of REA must be larger than the microscopic characteristic length of the porous medium to avoid rapid small-scale fluctuations, and must also be smaller than the characteristic length of the large-scale inhomogeneities [13, 34].

The statistical mechanics developed by Hansen et al. for immiscible and incompressible two-phase flow in porous media [31], leading to a thermodynamics-like formalism for the macroscopic variables describing the flow [35–38], is reviewed in Section II. We go into some detail here in order to place the present work in a proper context.

The dynamic pore network model [39, 40] used in this work is introduced in Section III. The model is implemented as a two-dimensional lattice where the REA is defined as a one-dimensional sub-lattice placed orthogonally to the average flow direction.

The aim of this paper is to demonstrate that Equation (4) is valid for our dynamic pore network model. This equation states that the statistics of the variables characterizing the REA do not depend on the statistics of the reservoir apart from local interactions. We report on our findings in Section IV. We first investigate how the statistics of the variables we focus on, the wetting saturation and the Darcy velocity, vary with the size of the sub-lattice we consider, see Subsection IV A. This allows us to determine when the sub-lattice is large enough to

act as an REA. We then proceed to study the dependence of the variable fluctuations on the size of the REA in Subsection IV B. Surprisingly, whereas the fluctuations of the wetting saturation, scale as the inverse of the square root of the size of the REA, the average Darcy flow velocity fluctuations scale as the inverse of the size of the REA to the power 0.83. Lastly, in Subsection IV C we test whether the statistics measured in the REA are independent of the size of the reservoir. We do indeed find that this is, thus verifying the validity of Equation (4) for our dynamical pore network model.

A pertinent question is, what would happen if the verification of Equation (4) would have failed? It would invalidate the statistical mechanics of Reference [31], but it would also have a negative impact on any attempt at constructing a local theory for immiscible two-phase flow at the Darcy scale in that all quantities are local. Rather than having the theory represented in the form of differential equations, they would contain integrals over space. We summarize and discuss this in Section V in addition to the other results.

II. STATISTICAL MECHANICS

We review in the following the statistical mechanics approach to immiscible and incompressible two-phase flow in porous media of Hansen et al. [31]. Envision a homogeneous cylindrical block of porous medium as shown in Figure 1, with a volumetric flow rate Q flowing through it. This flow consists of two immiscible and incompressible fluids which are well mixed before entering the porous medium. Keeping the flow entering into the porous media constant creates a steady-state flow within the porous medium. By steady-state flow we mean that the macroscopic variables describing the flow remain constant or fluctuate around well-defined averages. It is important to note that this does not imply that the pore scale interfaces between the fluids remain static. Rather, at the scale of the fluid clusters, there may be strong activity where clusters form and break up. Steady-state flow is a concept that is defined at the macroscopic Darcy level, not at the pore level. We may split Q into the volumetric flow rate of the more wetting fluid, Q_w , and the volumetric flow rate of the less wetting fluid, Q_n , so that

$$Q = Q_w + Q_n. \quad (1)$$

The flow is dissipative and hence molecular entropy is produced. There is viscous dissipation and the motion of fluid interfaces and contact lines contains a dissipative element [41]. This means that there is a production of entropy as hydrodynamic motion is converted into thermal motion. The Jaynes maximum entropy principle should therefore not be applicable [30]. We now explain how we get around this hurdle.

There are three scales that stand out in porous media: the molecular scale, the pore scale and the Darcy scale. At the sub-pore scale, the dissipation dominates the flow

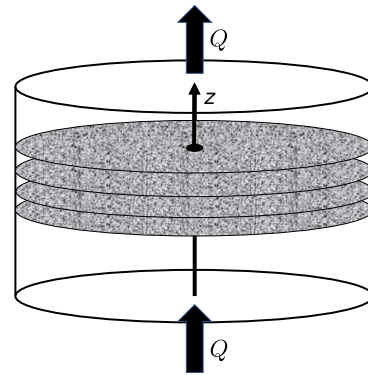


FIG. 1: A porous medium in the shape of a cylinder. There is a flow of volumetric flow rate Q passing through it. Four planes cutting through the cylinder orthogonally to the average flow direction, i.e., the z -axis, are shown. The volumetric flow rate Q is the same through each plane. However, the volumetric flow rate of each fluid, Q_w and Q_n vary from plane to plane.

and methods from non-equilibrium thermodynamics are appropriate [19–21]. However, on scales above the pore scale, it is the fluid clusters and how they move that dominate. One may associate an entropy with these fluid structures.

In order to construct this *flow entropy*, we imagine a cylindrical porous plug as shown in Figure 1. There is immiscible two-phase flow in the direction of the cylinder axis. We now focus on a set of imaginary planes that cut through the porous plug orthogonal to the cylinder axis as shown in Figure 1. Imagine each plane is divided into voxels with sufficient resolution. Each voxel is associated with a number of variables describing the flow through it. To be concrete, suppose we model the porous medium using the Lattice Boltzmann method (LBM) [42]. The voxels would then be the nodes of the lattice along the plane used in LBM and the variables would be the LBM variables associated with these nodes. The configuration in the plane, X , would be the values the voxel variables have at that particular instance in each voxel. Measuring over many configurations we may define a *configurational probability density* $P(X)$. This, in turn, defines our entropy,

$$\Sigma = - \int dX P(X) \ln P(X), \quad (2)$$

where the integral is over all *physically feasible configurations* in the plane. Note the important fact that since the structure of the porous matrix varies from plane to plane, this quenched disorder must be taken into account.

Before taking the next step, it is useful to think of the following system: We imagine a two-dimensional gas confined inside a box. The molecules of the gas move around incessantly. At a given moment, the position and velocity of each molecule will define an instantaneous gas configuration. The aim of statistical mechanics in this context is to provide the configurational probability den-

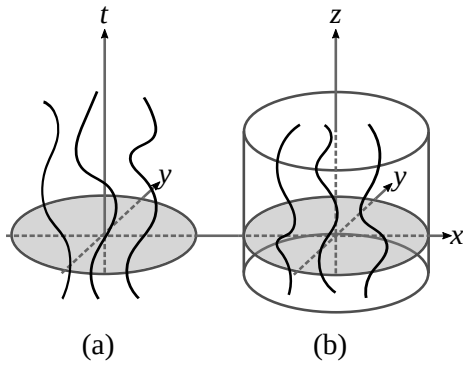


FIG. 2: We are illustrating to the left (a) the world lines of molecules in a two-dimensional gas in a space-time diagram. To the right (b), we show some streamlines of a fluid mixture flowing in a porous medium.

sity for these instantaneous configurations. There is no production of entropy in this system from the motion of the molecules. It is in equilibrium. However, we may represent the gas in a three-dimensional *space-time plot*, see Figure 2(a). Then, each molecule is represented by its world line and the configurations represent the world lines cutting through planes orthogonal to the time axis.

Figure 2(b) shows the streamlines of a fluid flowing through a porous medium. There is a striking analogy between these streamlines and the world lines of the molecules in the space-time plot of molecules of the two-dimensional gas, when we interpret the z -axis in Figure 2(b) as a “time” axis. Figure 7 in Reference [43] illustrates this point in more detail. Cuts through the porous medium as shown in Figure 1 are then analogous to the snapshots of configurations of the gas molecules taken at different times. The flow entropy defined in Equation (2) then corresponds to the entropy of the gas molecules, and as in the gas, there is no production of this flow entropy along the z -axis.

The volumetric flow rate Q has the same value for all planes orthogonal to the flow axis. Hence, with the flow axis acting as a “time” axis, Q is a conserved quantity along this axis. We may therefore interpret Q as being analogous to the internal energy of the two-dimensional gas. Note that neither Q_w nor Q_n are conserved, only their sum Q (Equation (1)) is. However, both have well-defined averages. The porous medium block of Figure 1 may be seen as an analog of a two-dimensional gas that does not exchange heat with its surroundings. In other words, it is the analog of a *microcanonical system*.

Figure 3 shows one of the planes cutting through the porous medium orthogonally to the flow direction, i.e., the z -axis. A sub-area of this plane that is large enough to reflect the behavior of the entire plane is chosen. Hence, this area acts as an REA [33]. We characterize this REA by three variables in addition to its total area A : Q_p the volumetric flow rate through it, A_p which is the area inside the REA covered by pores, and $A_{w,p}$ which is the part of the pore area that is covered by the

wetting fluid. The configurations within the REA we refer to as X_p . These configurations are a subset of the configurations X in the entire plane. Denoting X_r as the part of X which excludes the REA gives

$$X = X_r \cup X_p. \quad (3)$$

We now refer to the discussion in the Introduction (Section I) and interpret the REA as the *system* and the plane excluding the REA as the *reservoir*. For the Jaynes maximum entropy approach to be applicable, we must have that

$$P(X) = p_r(X_r)p(X_p), \quad (4)$$

where $p_r(X_r)$ is the configurational probability for the reservoir and $p(X_p)$ is the configurational probability for the REA. The significance of this equation is that it ensures that it is possible to consider the REA as an autonomous system that interacts with the reservoir. Without this property, a local description of the flow at the Darcy scale would then not be possible.

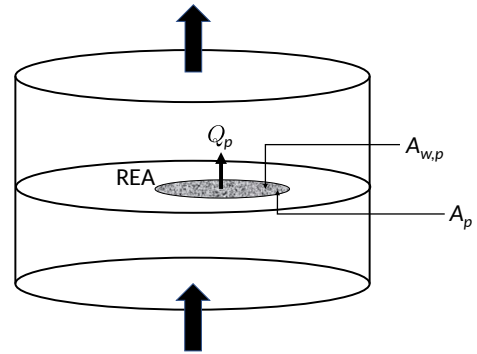


FIG. 3: Shows one of the planes cutting through the porous media block orthogonal to the flow direction which is upwards as marked with the arrows. In the plane, a sub-area that is large enough to reflect the behavior of the entire plane so that it acts as a Representative Elementary Area (REA) is selected. The REA is characterized by three variables besides its area A : The volumetric flow rate through it, Q_p , the area covered by the pores, A_p , and the area filled with the wetting fluid $A_{w,p}$.

It is the aim of this paper to verify the validity of Equation (4). This equation allows us to define a flow entropy for the REA,

$$\Sigma_p = - \int dX_p p(X_p) \ln p(X_p), \quad (5)$$

where the integral runs over all physically feasible configurations.

We maximize the entropy with the constraints that the averages of Q_p , A_p and $A_{w,p}$ are known. This gives [31]

$$p(X_p) = \frac{1}{Z} \exp \left[-\frac{Q_p(X_p)}{\theta} + \frac{\pi A_p(X_p)}{\theta} + \frac{\mu A_{w,p}(X_p)}{\theta} \right], \quad (6)$$

where the partition function Z is given by

$$Z(\theta, \pi, \mu) = \int dX_p e^{-Q_p(X_p)/\theta + \pi A_p(X_p)/\theta + \mu A_{w,p}(X_p)/\theta} . \quad (7)$$

Here $Q_p(X_p)$, $A_p(X_p)$ and $A_{w,p}(X_p)$ are the variable values for the REA configuration X_p . It is through these three variables that contact is made with the pore-scale physics since this is where the configuration X_p enters. Three parameters appear in this equation: 1. the *agitation* θ which plays a role similar to that of temperature (and we note that the name, which is a contraction of the words “agitation” and “temperature” has been chosen to emphasize that this is *not* a temperature), 2. the *flow pressure* π which is conjugate of the pore area A_p — and hence the porosity, and 3. the *flow derivative* μ which plays the role similar to the chemical potential and which is the conjugate to the wetting area $A_{w,p}$ and hence the wetting saturation $S_{w,p} = A_{w,p}/A_p$.

Equation (7) constitutes the scaling up from the microscopic level, in other words the pore level, to the Darcy level, since we may from it determine the values of the macroscopic variables. We have thus succeeded in turning the scale-up problem from being a physical one to the mathematical problem of integration in Equation (7). The macroscopic variables that ensue from this approach are related through a thermodynamics-like formalism with all its richness [31, 35].

In ordinary thermodynamics, one finds a set of *general* relations between the macroscopic variables. They stem either from the Euler theorem for homogeneous functions or from the Gibbs relation [44, 45]. The same applies to the present formulation of the two-phase flow problem. We sketch the approach in the following.

We define an average pore velocity $v_p = Q_p/A_p$ and an entropy density $\sigma_p = \Sigma_p/A_p$. The average pore velocity v_p depends on the flow entropy density σ_p and the wetting saturation $S_{w,p}$: $v_p = v_p(\sigma_p, S_{w,p})$. With these variables, we may construct an equivalent to the *Gibbs relation*,

$$dv_p = \theta d\sigma_p - \mu dS_{w,p} . \quad (8)$$

We do a Legendre transform of the average flow velocity v_p from $(\sigma_p, S_{w,p})$ to (σ_p, μ) as control variables, finding

$$\hat{v}_n(\sigma_p, \mu) = v_p(\sigma_p, \mu) - S_{w,p}(\sigma_p, \mu)\mu , \quad (9)$$

where we have defined the *thermodynamic non-wetting velocity* [35]

$$\hat{v}_n = \left(\frac{\partial Q_p}{\partial A_{n,p}} \right)_{A_{w,p}, \sigma} . \quad (10)$$

There is also the *thermodynamic wetting velocity*

$$\hat{v}_w = \left(\frac{\partial Q_p}{\partial A_{w,p}} \right)_{A_{n,p}, \sigma} . \quad (11)$$

The non-wetting area $A_{n,p}$ is the area of the REA that is covered by the non-wetting fluid. We furthermore have that

$$S_{w,p} = - \left(\frac{\partial \hat{v}_n}{\partial \mu} \right)_{\sigma} , \quad (12)$$

and

$$\mu = - \left(\frac{\partial v_p}{\partial S_{w,p}} \right)_{\sigma} . \quad (13)$$

Equations (9) through (13) demonstrate the power of this approach. These relations are far from obvious.

There is one more central aspect that needs to be brought to light. The thermodynamic velocities defined in Equations (10) and (11) are *not* the pore velocities of the fluids

$$v_w = \frac{Q_{w,p}}{A_{w,p}} , \quad (14)$$

and

$$v_n = \frac{Q_{n,p}}{A_{n,p}} , \quad (15)$$

where $Q_p = Q_{w,p} + Q_{n,p}$ in analogy with Equation (1). Rather, they are related through the two equations [35–37]

$$v_w = \hat{v}_w - S_{w,p}v_m , \quad (16)$$

$$v_n = \hat{v}_n + S_{n,p}v_m , \quad (17)$$

where $S_{n,p} = A_{n,p}/A_p = 1 - S_{w,p}$ and v_m is the *co-moving velocity*. It turns out from experimental and numerical data that the co-moving velocity is extraordinarily simple [37],

$$v_m = a(\sigma) + b(\sigma)\mu , \quad (18)$$

where $a(\sigma)$ and $b(\sigma)$ are functions of the flow entropy density. There is no equivalent to the co-moving velocity in ordinary thermodynamics [38].

Calculating the partition function $Z(\theta, \pi, \mu)$ defined in Equation (7) requires a knowledge of the pore-scale configurations X_p through the three variables $Q_p(X_p)$, $A_p(X_p)$ and $A_{w,p}(X_p)$. Furthermore, the integral runs only over physically feasible configurations. As already mentioned, this is where the characteristics of a given porous medium and the fluids enter. It is here details of the pore scale physics enters, such as interfacial tension gradients and interface curvature at the fluid-fluid interfaces. This is where contact is made between this theory and the ongoing research on the pore-scale physics of immiscible two-phase flow.

III. DYNAMIC PORE NETWORK MODEL

In order to explore the validity of Equation (4), we use a dynamic pore network model [40, 46] originally developed by Aker et al. [39] and then further developed

in e.g., [47–53], including direct comparison with experimental systems, [54, 55]. In the latter of these two references, the performance of the model is also compared to other models.

We illustrate the model as it is implemented in the context of the present paper in Figure 4. We use a square lattice where the links represent single pores, all having the same length l , but with a distribution in their radii. The lattice has dimensions $L_x \times L_y$ measured in units of l , and we implement periodic boundary conditions in both the flow direction and the transversal direction. The square lattice is oriented at 45° angle with respect to the average flow direction.

The links connecting neighboring nodes contain the pore throats. The nodes have no volume associated with them. The variation in the cross-sectional area of the pore throat and pore bodies are modeled by an hourglass shape so that a fluid meniscus in link i will generate a capillary pressure according to the Young-Laplace Equation [3]

$$p_{c,i}(x) = \frac{2\gamma \cos \theta}{r_i(x)}, \quad (19)$$

where $x \in [0, l]$ is the position of the interface along the center axis of the link, having a length l . Here γ is the surface tension and θ is the wetting angle measured through the wetting fluid which is the fluid that has the smallest angle with the solid wall. We note that this expression is only valid under hydrostatic conditions. Hence, using it in a dynamic setting implies the assumption that the motion of the interfaces is slow. This assumption is difficult to justify during Haines jumps. We still use it as an approximation that enters together with all the other approximations that the model requires. We furthermore ignore hysteretic effects associated with the wetting angle with the same justification as for using the Young-Laplace equation. The variable indicating the shape of the link in Equation (19) is the radius of the link at position x , which is given by

$$r_i(x) = \frac{r_{0,i}}{1 - c \cdot \cos\left(\frac{2\pi x}{l}\right)}, \quad (20)$$

where c is the amplitude of the variation and r_0/c is randomly chosen from the interval $[0.1l, 0.4l]$, thus creating a disorder in the properties of the network.

The fluids within a given link are pushed with a force caused by the total effective pressure across it which is the difference between the pressure drop between the two nodes it is attached to, Δp , and the total capillary pressure $\sum_k p_c(x_k)$ due to all the interfaces with positions $x_k \in [0, l]$. The model has been set to allow up to four interfaces in each link, and this necessitates merging of the interfaces as described in [40].

The constitutive relation between the volumetric flow rate q_i through link i and pressure drop Δp_i across the

same link is [40, 56]

$$q_i = -\frac{\pi \bar{r}_i^4}{8\mu_i l} \left(\Delta p_i - \sum_k p_{c,i}(x_k) \right), \quad (21)$$

where \bar{r}_i is the average hydraulic radius along the link. Furthermore, we have that $\mu_i = s_{w,i}\mu_{w,i} + s_{n,i}\mu_{n,i}$ is the saturation-weighted viscosity of the fluids in link i where $s_{w,i} = V_{w,i}/V_i$ and $s_{n,i} = V_{n,i}/V_i$ are the saturations of the wetting fluid and the non-wetting fluid respectively with viscosities $\mu_{w,i}$ and $\mu_{n,i}$, and volumes $V_{w,i}$, $V_{n,i}$, and $V_i = \pi \bar{r}_i^2 l$.

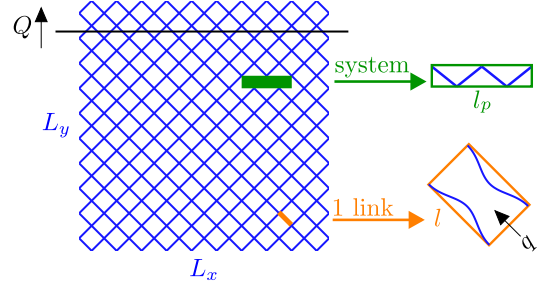


FIG. 4: Two dimensional dynamic pore network model with dimensions $L_x \times L_y$ links consists of hourglass shaped links with length l and volumetric flow rate q passing through them, oriented 45° from the average flow direction. The total volumetric flow rate Q is constant over all the cross sections normal to the average flow direction. An example of a “system” with length $l_p = 4$ links is marked, and the rest of the network surrounding the system is the “reservoir.”

In order to calculate the flow through the links and move the interfaces correspondingly, we solve the Kirchhoff for the network using a conjugate gradient algorithm [57]. Our numerical precision in determining the flow rates is 10^{-6} .

Using the terminology introduced in the Introduction, we divide the network into a “system”, corresponding to the REA, and a “reservoir” which is the rest of the network. The systems are chosen as illustrated with an example in Figure 4 where the system is placed orthogonally to the flow direction, i.e., in the same way as in Figure 3. Systems are made up of l_p number of links, for instance, the system in Figure 4 has $l_p = 4$ links. The pore area A_p of a system is the sum of the transverse area, the area orthogonal to the total flow direction, of each link belonging to that system,

$$A_p = \sum_{i=1}^{l_p} \sqrt{2} \pi (\bar{r}_i)^2, \quad (22)$$

where $\sqrt{2} = 1/\cos(45^\circ)$ comes from the fact that links in the model are oriented in 45° angle from the flow direction. Similarly, the total wetting fluid pore area of the system $A_{w,p}$ is the sum of the product of the transverse

area and the wetting fluid saturation in each link,

$$A_{w,p} = \sum_{i=1}^{l_p} \sqrt{2\pi}(\bar{r}_i)^2 s_{w,i} . \quad (23)$$

The volumetric flow rate through a system with l_p links is

$$Q_p = \sum_{i=1}^{l_p} q_i , \quad (24)$$

and its wetting saturation is

$$S_{w,p} = \frac{A_{w,p}}{A_p} . \quad (25)$$

IV. NUMERICAL INVESTIGATIONS

The simulations start from a random distribution of fluids within the network. The model is then integrated forwards in time while monitoring the pressure drop across it. When the pressure drop settles to a well-defined and stable average value, the model has reached steady-state flow. At this point, 20 system locations are chosen randomly at every 100th time-iteration, to get measurements that are mostly uncorrelated in time and space. Within each of these systems, the values of Q_p/l_p and $S_{w,p}$ are measured. This procedure ensures averaging not only over the motion of the fluids but also over the disorder of the porous medium itself. This process is repeated for a time corresponding to the passing of approximately 25 pore volumes of fluid through the model, where pore volume is the total volume of the links in the model. We do this for different widths l_p for the systems. In addition, the changes in the model size are studied by testing various model widths L_x while keeping the total length of the model fixed at $L_y = 60$ links. The links in the model are all $l = 1$ mm long. The two immiscible fluids have $\gamma = 3.0 \cdot 10^{-5}$ N/mm, $\mu_w = \mu_{nw} = 0.1$ Pa·s and $\theta = 70^\circ$. The overall wetting saturation for the network is fixed at $S_w = 0.5$. Due to the periodic boundary conditions, the volume of the fluids is conserved and the total saturation is constant. The total volumetric flow rate per unit width of the network is fixed at $Q/L_x = 0.7$ mm³/(s·link). The capillary number can be calculated from $Ca = \mu Q/(\gamma A_{\text{tot}})$ where A_{tot} is the total cross sectional area [40], giving $Ca \approx 0.012$.

A. System Variable Statistics

Figures 5 and 6 show box plots of $S_{w,p}$ and Q_p/l_p as functions of l_p , for a network with dimensions 120×60 links². In each box plot, the lower edge of the box which we can denote b_1 , the center line (median) b_2 and the upper edge b_3 correspond to the 25th, 50th and 75th

percentiles of the data, respectively. The lower and upper limits that exclude the outliers are $b_1 - 1.5(b_3 - b_1)$ and $b_3 + 1.5(b_3 - b_1)$, respectively.

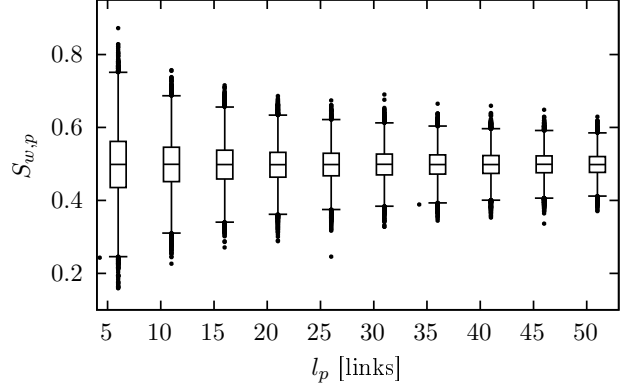


FIG. 5: Box plots showing the wetting fluid saturation $S_{w,p}$ in systems with width l_p . The model has dimensions 120×60 links².

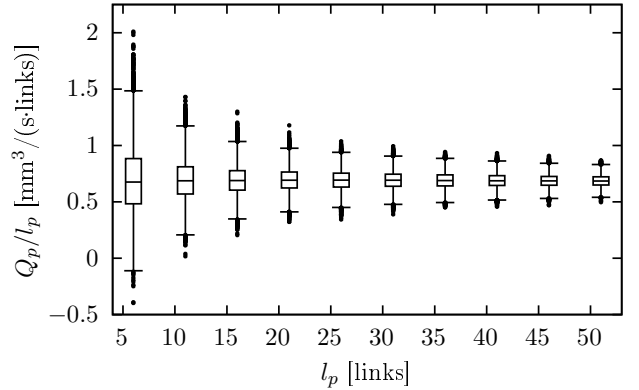


FIG. 6: Box plots showing the volumetric flow rate per unit system-width Q_p/l_p in systems with width l_p . The model has dimensions 120×60 links².

Since the control parameters for the entire network are fixed at $S_w = 0.5$ and $Q/L_x = 0.7$ mm³/(s·link), the average values $\langle S_{w,p} \rangle$ and $\langle Q_p/l_p \rangle$ in the systems will be the same as these values if measured with large enough statistics while the fluctuations around them will depend on l_p . In Figures 5 and 6, the medians for all system sizes, l_p , agree well with these expected average values. This factor indicates the existence of REAs since the intensive quantities inside REA must have well-defined averages that are independent of the size of the REA. This agreement is even true for systems as small as $l_p = 6$ links.

Furthermore, both Figures 5 and 6 show a steady decrease in the variations in the distributions with increasing l_p as the edges of the boxes approach the medians. This is more prominent for Q_p/l_p in Figure 6 than for $S_{w,p}$ in Figure 5. This is a reflection of Q/L_x being constant for any cut through the model orthogonally to the

average flow direction, since $Q_p/l_p \rightarrow Q/L_x$ as $l_p \rightarrow L_x$. On the other hand, $S_{w,p}$ has no such restrictions and is therefore allowed to fluctuate, even when $l_p = L_x$. The fact that there is a smaller spread in both distributions with increased l_p is another factor that signals possible REAs.

B. Size Dependence of Fluctuations

One way to quantitatively study the fluctuations in $\xi \in \{S_{w,p}, Q_p/l_p\}$ is through their corrected standard deviations given by [58]

$$\delta\xi = \sqrt{\frac{\sum_i^N (\xi_i - \langle\xi\rangle)^2}{N-1}} \quad (26)$$

where N is the number of measurements and $\langle\xi\rangle = (\sum_i^N \xi_i)/N$ is the mean. The standard deviations of $S_{w,p}$ and $\delta Q_p/l_p$ as a function of the system width l_p are shown in Figures 7 and 8, respectively.

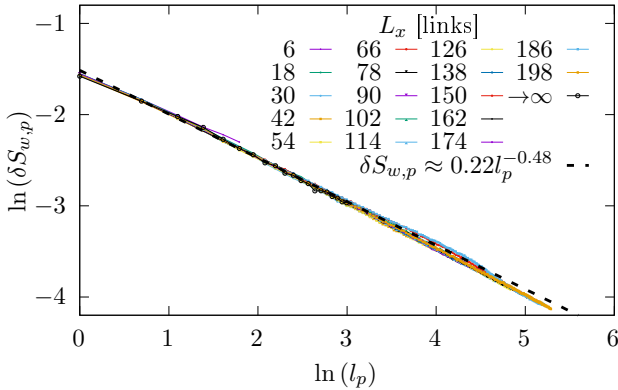


FIG. 7: Standard deviation of the wetting fluid saturation $S_{w,p}$ in systems with widths l_p residing in models having widths L_x and length 60 links.

We note the difference in behavior in Figures 7 and 8 in that $\delta Q_p/l_p$ drops off dramatically when l_p approaches L_x whereas no such effect is seen for $\delta S_{w,p}$. This is caused by the fact that Q is not fluctuating in the planes orthogonal to the average flow direction, whereas there is no such constraint for S_w , which is a factor also mentioned earlier. To avoid the measurements taken inside the systems being affected by the boundary effects, REA needs to be adequately smaller than the total model.

We also show in Figures 7 and 8 the results of extrapolation to infinitely large model $L_x \rightarrow \infty$. To understand how this was calculated, start by looking at Figure 9 where the results from Figures 7 and 8 have been plotted in a different way. In order to extrapolate to $L_x \rightarrow \infty$, the simulation results used must be from cases where the systems are much smaller than the model. To comply with this, the extrapolation process was performed for

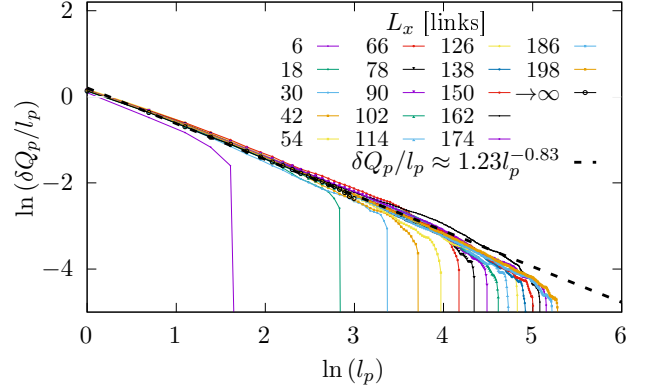


FIG. 8: Standard deviation of the volumetric flow rate per unit system width $\delta Q_p/l_p$ in systems with widths l_p residing in models with widths L_x and length 60 links.

$l_p \in [1, 20]$ links and $L_x \in [150, 198]$ links. For these values of l_p and L_x , Figure 9 shows that there is a linear relationship between $\delta\xi \in \{\delta S_{w,p}, \delta Q_p/l_p\}$ and $1/L_x$. Therefore, linear regression fit of the form

$$\delta\xi = \frac{c_1}{L_x} + \delta\xi_\infty, \quad (27)$$

can be performed for each l_p , where c_1 and $\delta\xi_\infty$ are constants. It can be observed from Equation (27) that $\delta\xi \rightarrow \delta\xi_\infty$ when $L_x \rightarrow \infty$, hence $\delta\xi_\infty$ are the extrapolation results. In Figure 9, $\delta\xi_\infty$ are the intersections the linear fits in Equation (27) make with the vertical axis.

After obtaining estimates for $\delta\xi_\infty$ for each l_p , we do a power law fit

$$\delta\xi_\infty = c_2 l_p^{-\beta} \quad (28)$$

to model the relationship between $\delta\xi_\infty$ and l_p where c_2 is a constant and β is an exponent. The result is

$$\lim_{L_x \rightarrow \infty} \delta S_{w,p} \approx 0.22 l_p^{-0.48} \quad (29)$$

for Figure 7 and

$$\lim_{L_x \rightarrow \infty} \left(\frac{\delta Q_p}{l_p} \right) \approx 1.23 l_p^{-0.83} \quad (30)$$

for Figure 8.

Based on the central limit theorem, the standard deviation of the average of l_p equally distributed independent variables is proportional to $l_p^{-1/2}$. The quantities $S_{w,p}$ and Q_p/l_p are both intensive quantities representing averages in l_p . We note from Equation (29) that this is the case with $S_{w,p}$, which could indicate that samples are uncorrelated. However, that the fluctuations $\delta Q_p/l_p$ in Equation (30) scales as one over l_p to the power 0.83 is a surprise presumably indicative of the samples being non-zero correlated in such a way that they fall off faster than when there are no correlations. This further means that the reservoir should be larger than the spatial correlation length for the systems to be not affected by finite-size effects.

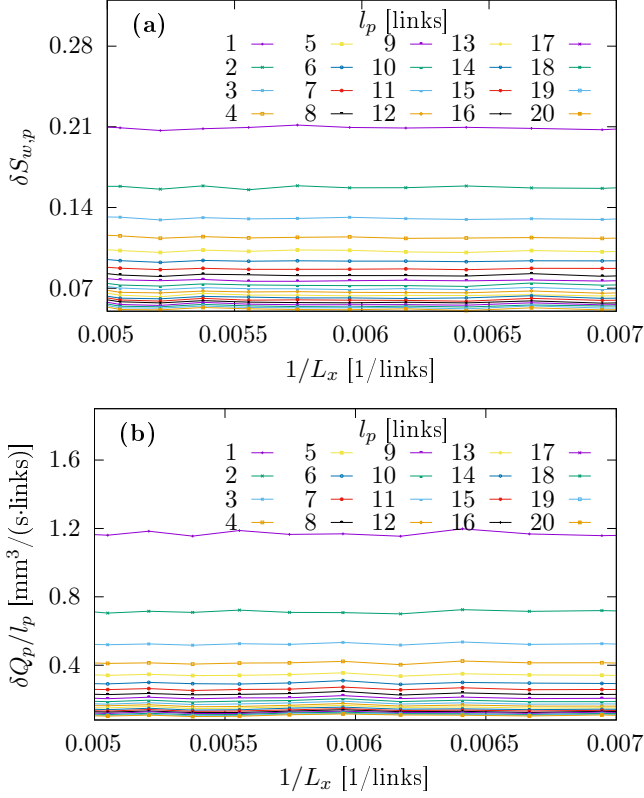


FIG. 9: Standard deviation of (a) the wetting fluid saturation $S_{w,p}$ and (b) the volumetric flow rate per unit system width Q_p/l_p in systems with widths l_p residing in models having widths L_x and length 60 links.

C. Reservoir Independence

We have now reached the central aim of this paper: Testing the validity of Equation (4) for our dynamic pore network model. This is done by keeping l_p fixed and varying L_x while monitoring histograms of $S_{w,p}$ and Q_p/l_p . If Equation (4) is valid for this model, the histograms should be independent of the model size L_x for large enough L_x .

The normalized histograms of $S_{w,p}$ and Q_p/l_p , measured for systems of width $l_p = 20$ links, are shown in Figures 10 and 11 respectively. We have split the two figures into two sub figures each in order to increase readability. Figures 10(a) and 11(a) show the normalized histograms for L_x being close to l_p , whereas Figures 10(b) and 11(b) show the normalized histograms for L_x much larger than l_p .

The normalized histograms for $S_{w,p}$ in Figure 10 seem to overlap for essentially all values of L_x . This effect can also be seen in the standard deviations in Figure 7 where $\delta S_{w,p}$ approximately follows Equation (29) regardless of the model size L_x or the system size l_p . This means, in the case of $S_{w,p}$, the reservoir independence seems to be satisfied regardless of the difference between l_p and L_x .

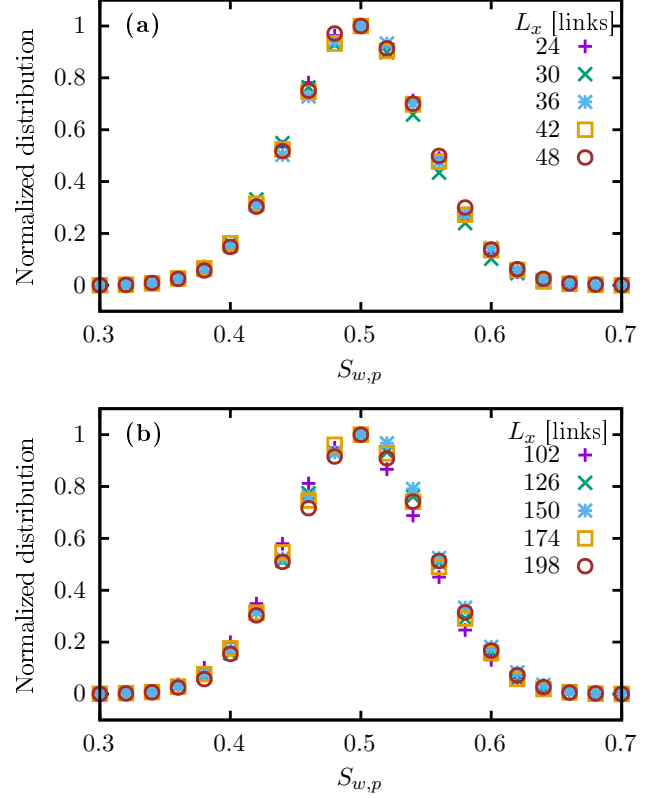


FIG. 10: Normalized histogram for the wetting fluid saturation $S_{w,p}$ in systems with width $l_p = 20$ links. The model has length 60 links and widths L_x that are close to l_p in (a) and are much larger than l_p in (b).

On the other hand, the histograms of Q_p/l_p differ more from each other when L_x is close to l_p , see Figure 11(a), compared to L_x being much larger than l_p where they overlap significantly larger, see Figure 11(b). This behavior is reflected in the standard deviation results in Figure 8 as well where $\delta Q_p/l_p$ following Equation (30) only when l_p is less than L_x . From these findings, we conclude that Q_p/l_p is independent of the reservoir size when L_x is sufficiently larger than l_p . This difference in behavior is presumably related to the flow rate Q/L_x being constant in all layers whereas the wetting saturation S_w fluctuates.

The results combined indicate that reservoir independence is valid for our model when the reservoir is adequately larger than the system.

V. CONCLUSION

The aim of this paper has been to address the plausibility of a necessary condition for the Jaynes statistical mechanics formulation [27] to be applicable to immiscible and incompressible two-phase flow in porous media. The condition demands that a such porous medium can be split into a system, functioning as a Representative

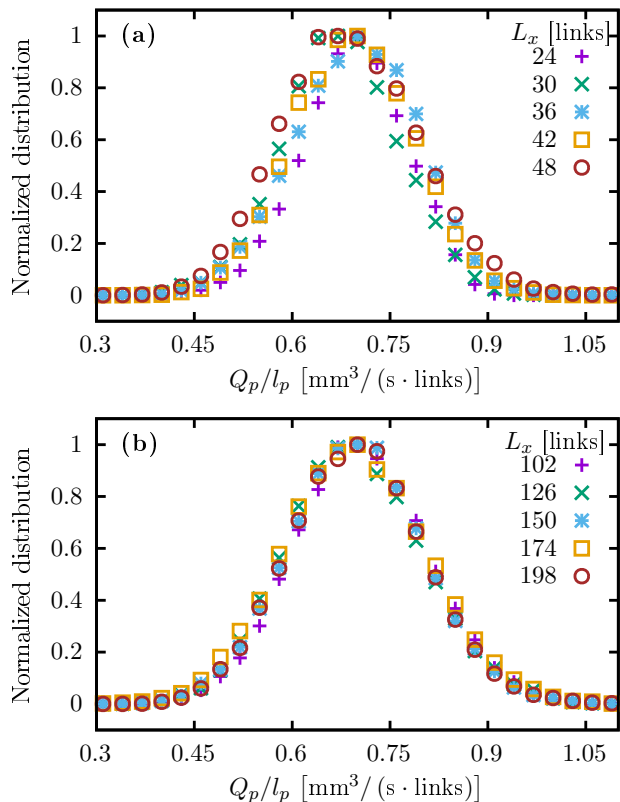


FIG. 11: Normalized histogram for the volumetric flow rate per link Q_p/l_p in systems width $l_p = 20$ links. The model has length 60 links and widths L_x that are close to l_p in (a) and are much larger than l_p in (b).

Elementary Area (REA), and a reservoir as in ordinary thermodynamics. This requires the statistics of the system to be independent of the size of the reservoir. Using dynamic pore network model simulations, we studied this by measuring distributions of key parameters using systems and reservoirs with different sizes.

First, the results show that there exist systems that can qualify as REAs within which the studied distributions have small spread and have well defined averages independent of the size of the REAs.

Second, REAs exhibit reservoir independence as demonstrated in Figures 10 and 11. Hence, the central Equation (4)

$$P(X) = p_r(X_r)p(X_p),$$

works for the dynamic pore network model.

As was alluded to at the end of the Introduction, the importance of the validity of Equation (4) goes beyond verifying the Jaynes statistical mechanics framework [31]. If Equation (4) would have failed, any attempt at constructing a local theory for immiscible two-phase flow at the Darcy scale would be in jeopardy. By local we mean that we can define variables that depend on a given point

in the porous medium and the theory then provides relations between these variables depending only on that point. Relative permeability theory is an example of such a local theory. A failure of Equation (4) would presumably necessitate the relations between variables containing integration over space.

When the reservoir size approaches to infinity, as the extrapolation results show, the fluctuations in the wetting fluid saturation depend on the system size through an exponent of -0.48 . The same exponent in the case of volumetric flow rate per unit system width is -0.83 . The fact that at least one of the fluctuations corresponds to an exponent significantly different from $-1/2$ indicates a non-zero spatial correlation between the links in the network, according to the central limit theorem. We speculate that this may be a consequence of total volumetric flow rate in the planes orthogonal to the average flow direction being a conserved quantity, whereas saturation in the same planes is not.

The measured distributions of saturation and volumetric flow rate inside systems are more similar when reservoir is much larger than system than when system and reservoir are closer in size. The cases with similar distributions indicate that reservoirs in these cases are adequately larger than the spatial correlation length for the systems to be unaffected by finite-size effects. Reservoir independence can be said to be achieved in these cases.

Our dynamic pore network model is capable of modeling porous media with a large number of pores (links). This comes at the cost of a simplified description of the structure of the pores and the motion of the fluids. Other models such as the Lattice Boltzmann Model [42] are capable of modeling the structure of the pores and the motion of the fluids inside them quite accurately. However, the price for this is the number of pores that may be modeled is limited. Nevertheless, attempts should be made to test reservoir independence of the systems also within the limits of this model. Another formidable task would be to analytically derive reservoir independence using hydrodynamics at the pore level.

VI. DECLARATIONS

Author Contributions: All the authors contributed in developing the theory and the methodology and writing the manuscript to its final form. HF performed the numerical simulations and data analysis. HF and SS wrote the code for the model.

Funding: This work was supported by the Research Council of Norway through its Center of Excellence funding scheme, project number 262644.

Acknowledgment: The authors thank Carl Fredrik Berg, Eirik G. Flekkøy, Daan Frenkel, Federico Lanza, Håkon Pedersen and Per Arne Slotte for interesting discussions.

- [1] J. Bear, *Dynamics of Fluids in Porous Media* (Dover, Mineola, 1988).
- [2] M. Sahimi, *Flow and Transport in Porous Media and Fractured Rock: from Classical Methods to Modern Approaches*, (Wiley, New York, 2011).
- [3] M. J. Blunt, *Multiphase Flow in Permeable Media* (Cambridge Univ. Press, Cambridge, 2017).
- [4] J. Feder, E. G. Flekkøy and A. Hansen, *Physics of Flow in Porous Media* (Cambridge University Press, Cambridge, 2022).
- [5] R. D. Wyckoff and H. G. Botset, *The flow of gas-liquid mixtures through unconsolidated sands*, *Physics* **7**, 325 (1936); doi.org/10.1063/1.1745402.
- [6] M. C. Leverett, *Capillary Behavior in Porous Sands*, *Trans. AIMME*, **12**, 152 (1940); doi.org/10.2118/941152-G.
- [7] S. Whitaker, *Flow in porous media II: The governing equations for immiscible, two-phase flow*, *Transp. Por. Med.* **1**, 105 (1986); doi.org/10.1007/BF00714688.
- [8] J. -L. Auriault and E. Sanchez-Palencia, *Remarques sur la loi de Darcy pour les écoulements biphasiques en milieu poreux*, *Journal of Theoretical and Applied Mechanics*, Numéro Spécial, 141 (1986).
- [9] J. -L. Auriault, *Nonsaturated deformable porous media: quasistatics*, *Transp. Porous Media*, **2**, 45 (1987); doi.org/10.1007/BF00208536.
- [10] J. -L. Auriault, O. Lebaigue and G. Bonnet, *Dynamics of two immiscible fluids flowing through deformable porous media*, *Transp. Porous Media*, **4**, 105 (1989); doi.org/10.1007/BF00134993.
- [11] D. Picchi and I. Battiato, *The Impact of pore-scale flow regimes on upscaling of immiscible two-phase flow in porous media*, *Water Res. Res.* **54**, 6683 (2018); doi.org/10.1029/2018WR023172.
- [12] D. Lasseux and F. J. Valdés-Parada, *A macroscopic model for immiscible two-phase flow in porous media*, *J. Fluid Mech.* **944**, A43 (2022); doi.org/10.1017/jfm.2022.487.
- [13] M. Hassanizadeh and W. G. Gray, *General conservation equations for multi-phase systems: 1. Averaging procedure*, *Adv. Water Resources* **2**, 131 (1979); doi.org/10.1016/0309-1708(79)90025-3.
- [14] S. M. Hassanizadeh and W. G. Gray, *Mechanics and thermodynamics of multiphase flow in porous media including interphase boundaries*, *Adv. Water Res.* **13**, 169 (1990); doi.org/10.1016/0309-1708(90)90040-B.
- [15] S. M. Hassanizadeh and W. G. Gray, *Towards an improved description of the physics of two-phase flow*, *Adv. Water Res.* **16**, 53 (1993); https://doi.org/10.1016/0309-1708(93)90029-F.
- [16] S. M. Hassanizadeh and W. G. Gray, *Thermodynamic basis of capillary pressure in porous media*, *Water Resour. Res.* **29**, 3389 (1993); doi.org/10.1029/93WR01495.
- [17] J. Niessner, S. Berg and S. M. Hassanizadeh, *Comparison of two-phase Darcy's law with a thermodynamically consistent approach*, *Transp. Por. Med.* **88**, 133 (2011); doi.org/10.1007/s11242-011-9730-0.
- [18] W. G. Gray and C. T. Miller, *Introduction to the thermodynamically constrained averaging theory for porous medium systems* (Springer Verlag, Berlin, 2014); doi.org/10.1007/978-3-319-04010-3.
- [19] S. Kjelstrup, D. Bedeaux, A. Hansen, B. Hafskjold and O. Galteland, *Non-isothermal transport of multi-phase fluids in porous media. the entropy production*, *Front. Phys.* **6**, 126 (2018); doi.org/10.3389/fphy.2018.00126.
- [20] S. Kjelstrup, D. Bedeaux, A. Hansen, B. Hafskjold and O. Galteland, *Non-isothermal transport of multi-phase fluids in porous media. Constitutive equations*, *Front. Phys.* **6**, 150 (2019); doi.org/10.3389/fphy.2018.00150.
- [21] D. Bedeaux and S. Kjelstrup, *Fluctuation-dissipation theorems for multiphase flow in porous media*, *Entropy*, **24**, 46 (2022); doi.org/10.3390/e24010046.
- [22] J. E. McClure, R. T. Armstrong, M. A. Berrill, S. Schlüter, S. Berg, W. G. Gray, and C. T. Miller, *Geometric state function for two-fluid flow in porous media*, *Phys. Rev. Fluids*, **3**, 084306 (2018); doi.org/10.1103/PhysRevFluids.3.084306.
- [23] R. T. Armstrong, J. E. McClure, V. Robins, Z. Liu, C. H. Arns, S. Schlüter and S. Berg, *Porous media characterization using Minkowski functionals: theories, applications and future directions*, *Transp. Porous Media*, **130**, 305 (2019); doi.org/10.1007/s11242-018-1201-4.
- [24] J. E. McClure, R. T. Armstrong and S. Berg, *Geometric evolution as a source of discontinuous behavior in soft condensed matter*, arXiv:1906.04073; doi.org/10.48550/arXiv.1906.04073.
- [25] J. E. McClure, M. Fan, S. Berg, R. T. Armstrong, C. F. Berg, Z. Li and T. Ramstad, *Relative permeability as a stationary process: Energy fluctuations in immiscible displacement*, *Phys. Fluids*, **34**, 092011 (2022); doi.org/10.1063/5.0107149.
- [26] F. Ravndal, *Scaling and Renormalization Groups*, No. INIS-MF-3303. Nordisk Inst. for Teoretisk Atomfysik (1976).
- [27] E. T. Jaynes, *Information theory of statistical mechanics*, *Phys. Rev.* **106**, 620 (1957); doi.org/10.1103/PhysRev.106.620.
- [28] C. E. Shannon, *A Mathematical theory of communication*, *The Bell System Technical Journal*, **27**, 379 (1948); doi.org/10.1002/j.1538-7305.1948.tb01338.x.
- [29] P. S. de Laplace, *A Philosophical Essay on Probabilities*, page 3 (Dover, New York, 1951).
- [30] L. F. Calazans and R. Dickman, *Steady-state entropy: A proposal based on thermodynamic integration*, *Phys. Rev. E*, **99**, 032137 (2019); doi.org/10.1103/PhysRevE.99.032137.
- [31] A. Hansen, E. G. Flekkøy, S. Sinha and P. A. Slotte, *A statistical mechanics for immiscible and incompressible two-phase flow in porous media*, *Adv. Water Resources*, **171**, 104336 (Elsevier, 2023); doi.org/10.1016/j.advwatres.2022.104336.
- [32] J. Xu and M. Y. Louge, *Statistical mechanics of unsaturated porous media*, *Phys. Rev. E*, **92**, 062405 (2015); doi.org/10.1103/PhysRevE.92.062405.
- [33] J. Bear and Y. Bachmat, *Introduction to Modeling of Transport Phenomena in Porous Media*, (Springer, Berlin, 2012); doi.org/10.1007/978-94-009-1926-6.
- [34] O. Rozenbaum and S. R. du Roscoat, *Representative elementary volume assessment of three-dimensional x-ray microtomography images of heterogeneous materials: Application to limestones*, *Phys. Rev. E*, **89**, 053304 (2014); doi.org/10.1103/PhysRevE.89.053304.

- [35] A. Hansen, S. Sinha, D. Bedeaux, S. Kjelstrup, M. A. Gjennestad and M. Vassvik, *Relations between seepage velocities in immiscible, incompressible two-phase flow in porous media*, Transp. Por. Med. **125**, 565 (2018); doi.org/10.1007/s11242-018-1139-6.
- [36] S. Roy, S. Sinha and A. Hansen, *Flow-area relations in immiscible two-phase flow in porous media*, Front. Phys. **8**, 4 (2020); doi.org/10.3389/fphy.2020.00004.
- [37] S. Roy, H. Pedersen, S. Sinha and A. Hansen, *The Co-moving Velocity in immiscible two-phase flow in porous media*, Transp. Por. Med., **143**, 69 (2022); doi.org/10.1007/s11242-022-01783-7.
- [38] H. Pedersen and A. Hansen, *Parametrizations of two-phase flow in porous media*, arXiv:2212.07285 (2022); doi.org/10.48550/arXiv.2212.07285.
- [39] E. Aker, K. J. Måløy, A. Hansen and G. G. Batrouni, *A two-dimensional network simulator for two-phase flow in porous media*, Transp. Porous Media, **32**, 163 (1998); doi.org/10.1023/A:1006510106194.
- [40] S. Sinha, M. Aa. Gjennestad, M. Vassvik and A. Hansen, *Fluid meniscus algorithms for dynamic pore network modeling of immiscible two-phase flow in porous media*, Front. Phys. **8**, 567 (2019); doi.org/10.3389/fphy.2020.548497.
- [41] N. R. Morrow, *Physics and thermodynamics of capillary action in porous media*, Ind. Eng. Chem., **62**, 32 (1970); doi.org/10.1021/ie50726a006.
- [42] T. Ramstad, C. F. Berg and K. Thompson, *Pore-scale simulations of single- and two-phase flow in porous media: Approaches and applications*, Transp. Porous Media, **130**, 77 (2019); doi.org/10.1007/s11242-019-01289-9.
- [43] M. Souzy, H. Lhuissier, Y. Méheust, T. Le Borgne and B. Metzger, *Velocity distributions, dispersion and stretching in three-dimensional porous media*, J. Fluid Mech. **891**, A16 (2020); doi.org/10.1017/jfm.2020.113.
- [44] H. B. Callen, *Thermodynamics as a science of symmetry*, Found. Phys. **4**, 423 (1974); doi.org/10.1007/BF00708519.
- [45] H. B. Callen, *Thermodynamics and an introduction to thermostatistics, 2nd Edition* (Wiley, New York, 1991); ISBN: 978-0-471-86256-7.
- [46] V. Joekar-Niasar and S. M. Hassanizadeh, *Analysis of fundamentals of two-phase flow in porous media using dynamic pore-network models: A review*, Critical Reviews in Environmental Science and Technology, **42**, 1895 (2012); doi.org/10.1080/10643389.2011.574101.
- [47] H. A. Knudsen, E. Aker and A. Hansen, *Bulk flow regimes and fractional flow in 2D porous media by numerical simulations*, Transp. Porous Media, **47**, 99 (2002); doi.org/10.1023/A:1015039503551.
- [48] T. Ramstad and A. Hansen, *Cluster evolution in steady-state two-phase flow in porous media*, Phys. Rev. E, **73**, 026306 (2006); doi.org/10.1103/PhysRevE.73.026306.
- [49] G. Tørå, P. E. Øren and A. Hansen, *A dynamic network model for two-phase flow in porous media*, Transp. Porous Media, **92**, 145 (2012); doi.org/10.1007/s11242-011-9895-6.
- [50] M. Aa. Gjennestad, M. Vassvik, S. Kjelstrup and A. Hansen, *Stable and efficient time integration of a dynamic pore network model for two-phase flow in porous media*, Front. Phys. **6**, 56 (2018); doi.org/10.3389/fphy.2018.00056.
- [51] M. Aa. Gjennestad, M. Winkler and A. Hansen, *Pore network modeling of the effects of viscosity ratio and pressure gradient on steady-state incompressible two-phase flow in porous media*, Transp. Porous Media, **132**, 355 (2020); doi.org/10.1007/s11242-020-01395-z.
- [52] M. Winkler, M. aa. Gjennestad, D. Bedeaux, S. Kjelstrup, R. Cabriolu and A. Hansen, *Onsager-symmetry obeyed in athermal mesoscopic systems: Two-phase flow in porous media*, Front. Phys. **8**, 60 (2020); doi.org/10.3389/fphy.2020.00060.
- [53] H. Fyhn, S. Sinha, S. Roy and A. Hansen, *Rheology of immiscible two-phase flow in mixed wet porous media: dynamic pore network model and capillary fiber bundle model results*, Transp. Porous Media, **139**, 491 (2021); doi.org/10.1007/s11242-021-01674-3.
- [54] S. Sinha, A. T. Bender, M. Danczyk, K. Keepseagle, C. A. Prather, J. M. Bray, L. W. Thrane, J. D. Seymour, S. L. Codd and A. Hansen, *Effective Rheology of Two-Phase Flow in Three-Dimensional Porous Media: Experiment and Simulation*, Transp. Porous Med. **119**, 77-94 (2017); doi.org/10.1007/s11242-017-0874-4.
- [55] B. Zhao, C. W. MacMinn, B. K. Primkulov, Y. Chen, A. J. Valocchi, J. Zhao, Q. Kang, K. Bruning, J. E. McClure, C. T. Miller, A. Fakhari, D. Bolster, T. Hiller, M. Brinkmann, L. Cueto-Felgueroso, D. A. Cogswell, R. Verma, M. Prodanovic, J. Maes, S. Geiger, M. Vassvik, A. Hansen, E. Segre, R. Holtzman, Z. Yang, C. Yuan, B. Chareyre and R. Juanes, *Comprehensive comparison of pore-scale models for multiphase flow in porous media*, Proc. Nat. Acad. Sci., **116**, 13799 (2019); doi.org/10.1073/pnas.1901619116.
- [56] E. W. Washburn, *The dynamics of capillary flow*, Phys. Rev. **17**, 273 (1921); doi.org/10.1103/PhysRev.17.273.
- [57] G. G. Batrouni and A. Hansen, *Fourier acceleration of iterative processes in disordered systems*, J. Statistical Phys. **52**, 747 (1988); doi.org/10.1007/BF01019728.
- [58] M. Stroeven, H. Askes and L. J. Sluys, *Numerical determination of representative volumes for granular materials*, Comp. Meth. Appl. Mech. Engn., **193**, 3221 (2004); doi.org/10.1016/j.cma.2003.09.023.